HHS Public Access

Author manuscript

Sci Signal. Author manuscript; available in PMC 2020 March 03.

Published in final edited form as:

Sci Signal. ; 11(521): . doi:10.1126/scisignal.aal4289.

Extension of chemotactic pseudopods by nonadherent human neutrophils does not require or cause calcium bursts

Emmet A. Francis, **Volkmar Heinrich***

Department of Biomedical Engineering, University of California Davis, Davis, CA 95616, USA.

Abstract

Global bursts in free intracellular calcium (Ca^{2+}) are among the most conspicuous signaling events in immune cells. To test the common view that Ca^{2+} bursts mediate rearrangement of the actin cytoskeleton in response to the activation of G protein–coupled receptors, we combined single-cell manipulation with fluorescence imaging and monitored the Ca^{2+} concentration in individual human neutrophils during complement-mediated chemotaxis. By decoupling purely chemotactic pseudopod formation from cell-substrate adhesion, we showed that physiological concentrations of anaphylatoxins, such as C5a, induced nonadherent human neutrophils to form chemotactic pseudopods but did not elicit Ca^{2+} bursts. By contrast, pathological or supraphysiological concentrations of C5a often triggered Ca^{2+} bursts, but pseudopod protrusion stalled or reversed in such cases, effectively halting chemotaxis, similar to sepsis-associated neutrophil paralysis. The maximum increase in cell surface area during pseudopod extension in pure chemotaxis was much smaller—by a factor of 8—than the known capacity of adherent human neutrophils to expand their surface. Because the measured rise in cortical tension was not sufficient to account for this difference, we attribute the limited deformability to a reduced ability of the cytoskeleton to generate protrusive force in the absence of cell adhesion. Thus, we hypothesize that Ca^{2+} bursts in neutrophils control a mechanistic switch between two distinct modes of cytoskeletal organization and dynamics. A key element of this switch appears to be the expedient coordination of adhesion-dependent lock or release events of cytoskeletal membrane anchors.

*Corresponding author. vheinrich@ucdavis.edu.

Author contributions: E.A.F. developed, performed, and analyzed the experiments and prepared the manuscript. V.H. developed, performed, and analyzed the experiments, prepared the figures and movies, and wrote the paper.

Competing interests: The authors declare that they have no competing interests.

SUPPLEMENTARY MATERIALS

www.sciencesignaling.org/cgi/content/full/11/521/eaal4289/DC1

Fig. S1. Dual-camera setup for simultaneous recording of bright-field and fluorescence images.

Fig. S2. Supraphysiological concentrations of C5a trigger Ca^{2+} bursts in resting human neutrophils without inducing chemotaxis.

Fig. S3. Concurrence of Ca^{2+} bursts and cellular contraction.

Fig. S4. Estimation of the cell surface area.

Fig. S5. Effective cortical tension during pure chemotaxis.

Movie S1. A Ca^{2+} burst in a human neutrophil.

Movie S2. Absence of Ca^{2+} bursts during complement-mediated, pure chemotaxis of a human neutrophil toward zymosan.

Movie S3. Absence of Ca^{2+} bursts during complement-mediated, pure chemotaxis of a human neutrophil toward β-glucan.

Movie S4. Supraphysiological concentrations of C5a or costimulation by shear flow can induce Ca^{2+} bursts in nonadherent human neutrophils.

INTRODUCTION

Calcium ions (Ca^{2+}) participate in many interactions between and within biomolecules. As a consequence, the cytoplasmic Ca^{2+} concentration in biological cells is an exceptionally potent effector of cellular behavior. Unlike the voltage-gated channels of electrically excitable cells, the Ca^{2+} channels of immune cells have long been thought to be actuated biochemically (1–6). In addition, flow chamber experiments have demonstrated that Ca^{2+} channels can also respond to mechanical stimulation of immune cells by shear flow (7–10).

Most of the existing work on Ca^{2+} signaling in immune cells has focused on the identification of channels and adapter molecules that regulate Ca^{2+} dynamics, and some studies have begun to address the molecular mechanisms that govern Ca^{2+} fluxes (11–18). The activation of heterotrimeric GTP-binding protein–coupled receptors (GPCRs) by chemoattractants (2–6, 16, 19–23) and the ligation of phagocytic (18, 24–30) or adhesive (7, 10, 11, 31) receptors have been implicated as primary causes of distinctive Ca^{2+} surges frequently observed in immune cells. However, although the involvement of adhesive and phagocytic receptors in such transient signaling bursts seems well established, the notion of a causal relationship between chemotactic GPCR activation and Ca^{2+} bursts conflicts with a small number of studies that have reported GPCR-mediated immune cell chemotaxis without such bursts (32, 33).

We used an interdisciplinary strategy to complement previous efforts by seeking to understand Ca^{2+} bursts in the context of their physiological role in critical immune processes. Questions of interest include, for example, the following: What are the original causes of Ca^{2+} bursts? When exactly do Ca^{2+} bursts occur, and why do they occur at those particular times? What are the major consequences of a Ca^{2+} burst, and which cellular functions depend on them? Such questions touch on the core of our understanding of immune cell behavior, yet they are rarely addressed in the literature and generally lack definitive answers. Our knowledge gaps are especially wide when it comes to the most important study subjects of immunology—humans—whose immune cells cannot be cultured or genetically manipulated.

We applied a single-live-cell, single-target assay (34–36) to examine intracellular Ca^{2+} concentrations during controlled one-on-one encounters between neutrophils—the most abundant type of human white blood cell—and pathogenic surfaces. Our results invite a careful reevaluation of some common assumptions about Ca^{2+} signaling in immune cells. Therefore, it is crucial to bear in mind the definitions and experimental conditions that underlie our results. First, all our experiments use human neutrophils. To ensure that all experiments start from a common baseline, we always strive to maintain the neutrophils in a nonadherent, initially quiescent state. We use the term “pure chemotaxis” to denote an autonomous cell deformation induced by a gradient of chemoattractant in the absence of adhesion to a substrate. In other words, we examined purely chemotactic recognition and protrusion in a manner that rules out interference or bias caused by substrate adhesion, which also eliminated the possibility that adhesive bonds or the application of a pulling force to these bonds might induce Ca^{2+} bursts in our experiments.

We define a Ca^{2+} burst as a rapid, global, and large increase of the intracellular Ca^{2+} concentration. In all experiments reported here, occurrences of these bursts were distinctive all-or-nothing events, meaning that the mean fluorescence intensity (MFI) corresponding to the intracellular Ca^{2+} concentration increased by at least a factor of 2.5 within a few seconds, in contrast to much smaller intensity changes that are slight in comparison. The present study focuses on Ca^{2+} bursts in the context of complement-mediated, pure chemotaxis. Although we frequently allowed neutrophils to phagocytose target particles at the end of single-live-cell experiments, the detailed analysis of this final stage is beyond the scope of this study. Relying on the well-established occurrence of Ca^{2+} bursts during phagocytosis (18, 23–26, 29, 30), we simply use the phagocytic stage as a built-in, per cell positive control.

Complement-directed chemotaxis is the predominant mechanism by which immune cells locate and home in on nearby pathogenic bacteria and fungi (37). As part of the host's innate immune defense, fragments of serum-based complement proteins assemble into proteases on recognized pathogen surfaces. These convertases cleave other complement proteins to produce and release small chemoattractant peptides called anaphylatoxins that stimulate chemotactic receptors on immune cells (38). Among the three anaphylatoxins (C5a, C3a, and C4a), the most potent inflammatory peptide is C5a (39). Its acute physiological relevance is underlined by its involvement in sepsis (40–44) and various other diseases (39). The physiological concentration of C5a is uncertain because it is difficult to quantify C5a separately from its less active, desarginated form C5a(desArg). Reported C5a concentrations in healthy donors ranging from 0.25 to 0.76 nM (45–47) usually represent the values of total concentrations of C5a and C5a(desArg) combined. Realistic estimates of the dynamics of C5a desargination reveal that C5a is rapidly metabo-lized by carboxypeptidases under physiological conditions and that appreciable amounts of C5a are expected to persist only within a thin anaphylatoxic cloud surrounding complement-recognized particles (37, 48). This implies that systemic physiological concentrations of C5a are actually extremely low, perhaps even negligible, as also supported by reports that picomolar C5a concentrations suffice to elicit a strong response by adherent neutrophils (49, 50). Here, we define "physiological concentration" in a simple empirical manner, based on the normal response of human neutrophils to nearby pathogenic targets under conditions where anaphylatoxins are produced and degraded naturally by the supplemented autologous donor serum.

RESULTS

Absence of Ca^{2+} bursts during complement-mediated, pure chemotaxis

Our pure chemotaxis assay uses micropipette manipulation or optical tweezers to maneuver bacterial, fungal, or surrogate target particles into the proximity of nonadherent, initially quiescent human neutrophils (36). If chemoattractants emanate from the target surface and stimulate a nearby neutrophil, then the neutrophil extends a chemotactic process toward the target. This morphological change is readily observed microscopically and serves as a straightforward readout of the neutrophil's chemotactic activity, as demonstrated for a selection of previously studied bacterial and fungal target pathogens (Fig. 1, A to C) (51,

52). Thus the neutrophils serve as ultrasensitive biode-tectors of minuscule amounts of chemoattractant produced at the target surface (Fig. 1D) (48).

In all cases where neutrophils extended chemotactic protrusions, this response required the presence of host serum in the medium, confirming that the chemoattractants inducing the neutrophil response did not originate from the targets themselves but were produced by the host's complement system. For bacterial targets such as *Salmonella enterica* serovar Typhimurium and *Escherichia coli*, the fungal targets *Coccidioides posadasii* and *Candida albicans*, and surrogate model particles made from cell walls of yeast (zymosan) or from microbial cell wall polysaccharides (β-glucan), this type of microbe-directed chemotaxis was predominantly mediated by the anaphylatoxin C5a (39, 51, 52). For example, blocking the C5a receptor CD88 or using C5-deficient serum diminished this chemotactic activity of neutrophils, and replacing the normal serum with heat-treated (at 52°C) autologous serum abolished it completely, although the neutrophils still phagocytosed the targets after physical contact (35, 51, 52). These findings confirm the broadly accepted view that C5a is the dominating chemoattractant in complement-mediated chemotaxis by neutrophils (39); however, other anaphylatoxins are also expected to participate in this process to some extent. Bearing in mind that all complement pathways result in the production of anaphylatoxins and assuming that the purely chemotactic neutrophil response examined in this study is common to all anaphylatoxins, we do not explicitly distinguish between different species of these chemoattractants here.

This study combines our pure-chemotaxis assay with fluorescent monitoring of the intracellular Ca^{2+} concentration of individual human neutrophils (Fig. 1E). A dual-camera setup allowed us to simultaneously record bright-field and fluorescence images of single-live-cell experiments (fig. S1 and Materials and Methods). The neutrophils were preloaded with the fluorescent Ca^{2+} dye Fluo-4, following a protocol that reduced the dye's side effects in the current setting as much as possible (Materials and Methods). To mimic interactions between complement proteins in the host serum and fungal pathogen surfaces, we used model particles of zymosan and β-glucan as targets in buffer supplemented with normal, autologous serum. These model targets are known to activate the complement cascade, which results in the production of C5a and other chemoattractant peptides (34, 35, 37, 48). Immunoglobulin G (IgG)–coated beads were used as a control. In each single-cell experiment, we first placed the particle near the neutrophil and observed the purely chemotactic neutrophil response for ~5 to 10 min and then placed the particle in contact with the cell.

In agreement with previous results (51), the neutrophils exhibited vigorous chemotactic activity in response to stimulation with zymosan or β-glucan particles but did not chemotax toward the IgG-coated beads (Fig. 2, A to C, and movies S1 to S3). All three target types readily adhered to the cells upon contact and triggered phagocytosis. We observed Ca^{2+} bursts in all experiments with targets of at least ~3 μm in diameter, independent of the type of target particle. In all cases, however, the Ca^{2+} burst occurred only after the target had been brought into contact with a neutrophil (Fig. 2, A to C), usually when phagocytosis was already underway. This final, phagocytic stage of our integrative recognition assay

confirmed that each neutrophil was viable and that the cell's Ca^{2+} signaling machinery was intact.

Each Ca^{2+} burst manifested as a rapid surge in fluorescence intensity that extended throughout the cell and exhibited similar features for all three target types (Fig. 2, D to F). Despite recording fluorescence images at 0.5-s intervals, using a camera exposure time of 100 ms or less, we never observed a gradual directional spreading of fluorescence across a cell. Instead, the fluorescence intensity increased throughout the neutrophil at about the same rate, reaching its peak within a few seconds. Unexpectedly, Ca^{2+} bursts never occurred during the earlier, pure-chemotaxis stage of our experiments with zymosan or β-glucan particles, even when cells were stimulated with clusters of β-glucan particles. Although the cells formed pronounced protrusions during this stage, variations in the measured MFI of Fluo-4 during pure chemotaxis were small and usually negligible compared to the surge of intensity observed later during phagocytosis (Figs. 1E and 2). Thus, under the near-physiological conditions used in these experiments, complement-mediated chemotaxis does not trigger global intracellular Ca^{2+} bursts in nonadherent human neutrophils. In other words, stimulation of the GPCRs of anaphylatoxins by physiological concentrations of their ligands alone is insufficient to induce Ca^{2+} bursts in situations such as those mimicked here. Moreover, the type of actin remodeling that accompanies the formation of purely chemotactic pseudopods neither requires nor causes Ca^{2+} bursts.

Anticorrelation of Ca^{2+} bursts and chemotactic protrusion

The observed absence of Ca^{2+} bursts during complement-mediated, pure chemotaxis of neutrophils agrees with a previous study that demonstrated neutrophil chemotaxis without Ca^{2+} bursts in a gradient of the chemotactic peptide *N*-formyl-Met-Leu-Phe (fMLP) (33), but the same study also reported that Ca^{2+} bursts did eventually occur when the chemotaxing neutrophils encountered very high concentrations of fMLP (33). Prompted by this observation, we tested whether we could force the occurrence of Ca^{2+} bursts by exposing nonadherent neutrophils to concentrations of C5a higher than those generated by the presence of zymosan or β-glycan particles in serum. We modified our dual-micropipetting system by replacing the target-holding pipette (the left pipette in Figs. 1 and 2) with a micropipette filled with a buffer containing C5a (53, 54), which allowed us to apply jets of C5a solutions to individual, nonadherent neutrophils.

Note that various issues handicap the unambiguous interpretation of this type of jet experiment. In short, the cells are not only stimulated by chemoattractant but also by fluid shear flow. Moreover, neither the concentration gradient of chemoattractant nor the fluid flow profile experienced along the cell surface are generally well known, in contrast to the clear picture established for single-cell, single-target experiments (Figs. 1 and 2) (37).

To determine whether high concentrations of C5a triggered Ca^{2+} bursts, we first subjected human neutrophils resting on the chamber bottom to jets of a 0.1 μM solution of C5a. All tested cells indeed responded to these C5a jets with strong bursts of Ca^{2+} (fig. S2), although the cells did not exhibit noticeable chemotactic deformations. Instead, cells that initially appeared smooth in microscopic images before the application of the C5a jet tended to

develop visible surface ruffles without any directional preference after the Ca^{2+} burst elicited by the C5a jet.

Next, we used our modified setup to apply C5a jets to pipette-held neutrophils (Fig. 3, A to C, and movie S4), varying the C5a concentration, jet pressure, and distance between the C5a pipette and the neutrophil to stimulate Ca^{2+} bursts in chemotactically active cells. It is important to bear in mind that the C5a concentration at the cell surface is lower than in the jet pipette due to the fluid flow profile and the metabolization of C5a by carboxypeptidases that are present in the autologous serum supplement in the chamber buffer. The observed neutrophil responses could be roughly categorized into three types (Fig. 3, A to C). In the first case (Fig. 3A), the cells responded to ~0.1 to 10 nM C5a solutions by extending pseudopods toward the source of C5a without generating Ca^{2+} bursts, replicating the behavior of neutrophils encountering target particles under the near-physiological conditions imposed in the previous experiments (Figs. 1 and 2). By contrast, Ca^{2+} bursts did occur in the other two cases (Fig. 3, B and C), usually after an increase of the C5a concentration or the jet pressure experienced at the cell surface. Almost all observed bursts exhibited similar features as described in the previous section, although in some instances (8 of 26 jet experiments that induced Ca^{2+} bursts), the fluorescence intensity was somewhat stronger in the pseudopod than in the rest of the cell.

The second type of neutrophil response was observed at C5a concentrations in the range of ~1 to 100 nM and comprised cases where pure chemotaxis was initiated before the Ca^{2+} burst occurred (Fig. 3B). In the third type of response, jets with a C5a concentration of ~0.1 μM or higher that were applied from a short distance induced Ca^{2+} bursts in neutrophils that did not form pronounced chemotactic protrusions (Fig. 3C). In both cases, the Ca^{2+} burst appeared to coincide with a noticeable neutrophil contraction in the axial direction defined by the cell and its holding pipette. Further analysis revealed that this axial cell contraction was indeed a common occurrence, observed in 24 of 26 cases of Ca^{2+} bursts (including cases of arrest of the axial cell extension; Fig. 4, A and B, and fig. S3). In a few experiments where we later retracted the C5a pipette or reduced the jet pressure, the cell recovered and resumed the protrusion of pseudopods [see time point labeled (5) in Fig. 3B and second example in movie S4], demon-strating that the contractile change in cell morphology was reversible. Although the concurrence of Ca^{2+} bursts and cellular contraction was often marked (fig. S3), these observations do not constitute definitive proof of a causal relationship between Ca^{2+} bursts and cell contraction. It is possible that a common original stimulus caused both the burst and the contraction in parallel, yet given that cell contraction and protrusion are opposing types of deformation, we can conclude that Ca^{2+} bursts and purely chemotactic protrusion are anticorrelated.

Two types of contractile force could govern the contractile change in cell morphology. One is the cortical tension, a force (per unit length) that acts tangential to the cell surface and opposes the expansion of the apparent surface area. The other is a normal force (per unit area) that acts to pull the cell surface inward in a perpendicular direction. If cortical tension dominated the cell contraction, then the resulting Laplace pressure would give rise to a smooth appearance of the cell surface and a cell projection into the cell-holding pipette that fills this pipette and ends in a hemispherical cap. If an inward-pulling force, on the other

hand, drove the cell contraction, then this would result in a rougher cell surface, including a cell projection in the cell-holding pipette that might pull away from the pipette wall and partially collapse. Careful inspection of our videomicrographs revealed a mixture of these morphological features, indicating that both types of force contributed to the observed cell contraction.

Limited cell deformation during pure chemotaxis

Although the above experiments confirmed that high concentrations of C5a triggered Ca^{2+} bursts in nonadherent neutrophils in vitro, it is unlikely that neutrophils encounter similarly high C5a concentrations in healthy humans. Therefore, it is unclear to what extent the observed contractile morphology contributes to the natural repertoire of neutrophil behavior. It seems plausible that it represents an exaggerated version of some particular aspect of a pre-programmed neutrophil response to anaphylatoxins. The mechanical nature of the cell contraction prompted us to also take a closer look at the mechanical features of the purely chemotactic cell response under near-physiological conditions where Ca^{2+} bursts do not occur (Figs. 1, 2, and 3A).

An intriguing difference between the cell deformations accompanying pure chemotaxis and those accompanying phagocytosis or cell migration became evident when we quantified the increase in the apparent cell surface area during the formation of purely chemotactic pseudopods. For comparison, human neutrophils are able to increase their apparent surface area to 250 to 300% of their initial resting surface area during osmotic swelling (55) or phagocytosis (51, 56). To establish how changes in surface area during pure chemotaxis compared to this value, we developed an image-analysis procedure that allowed us to estimate the cell surface area of neutrophils in suitable video images. Our analysis is based on the assumption that the visible two-dimensional (2D) outline of the cell represents a cross section of a rotationally symmetric 3D object and that this cross section contains the symmetry axis (fig. S4). This assumption seemed reasonable for many, but not all, video images. Images of cells that were too irregular to be approximated by a rotationally symmetric object were excluded from the analysis. We used this analysis to quantify the time course of the cell surface area changes during pure chemotaxis, as demonstrated for a neutrophil extending pseudopods toward a pipette-held zymosan particle (Fig. 5A), and to determine the maximum cell surface area during this process. In addition to our current experiments with target particles and C5a jets, we also estimated the maximum surface area increase of neutrophils during the formation of particularly large pseudopods from images of previous pure-chemotaxis experiments that were performed with various bacterial, fungal, and model targets without Fluo-4 imaging (Fig. 5B).

This analysis revealed that the cells rarely expanded their apparent surface area by more than ~25%, and never by more than 30%, during pure chemotaxis (Fig. 5B). This limit is much smaller—by a factor of ~8—than the maximum capacity of human neutrophils to expand their surface area (51, 56). However, this value coincides with the amount of mechanical slack exhibited by the cortex of these cells. Human neutrophils are known to accommodate surface area expansions of up to ~30% without having to cope with a significantly increased mechanical resistance (57). Larger changes of the surface area, however, require a much

stronger outward push by the cytoskeleton to overcome the rising cortical tension and other contractile forces (36, 57).

The limited ability of nonadherent neutrophils to expand their surface area could thus be due to insufficient protrusive force generation or prohibitive resistance by contractile forces. In view of the peculiar cell contraction induced by high concentrations of C5a (Figs. 3, B and C, and 4 and fig. S3), we next addressed whether physiological concentrations of anaphylatoxins might suffice to cause an abnormal rise of the cortical tension. Using a previously developed method (fig. S5A) (57, 58), we estimated the effective cortical tension during the formation of chemotactic pseudopods in the absence of Ca^{2+} bursts (fig. S5B). With very few exceptions, the measured tensions were within the expected range and consistent with the respective cell surface areas (fig. S5, B and C) (57). We therefore conclude that it is not an excessive cortical tension but a limited ability to generate protrusive force that prevents nonadherent neutrophils from expanding their surface area by more than ~30% during pure chemotaxis. The decisive prerequisite for larger surface expansions therefore appears to be cell adhesion to a substrate or target particle. A possible explanation for this requirement is the hypothesis that adhesive bonds anchor adjacent cytoskeletal filaments to the substrate or particle and nucleate a local increase in the rigidity of the cytoskeleton by promoting local actin cross-linking and polymerization. The resulting anchored and rigid cytoskeleton then provides the bracing support that is necessary for stronger protrusions of nonadherent patches of the cell surface.

DISCUSSION

Ca^{2+} bursts in immune cells represent a highly distinctive signaling mechanism that conducts a signal throughout the entire cell extremely rapidly. The return of the released Ca^{2+} into storage compartments such as calciosomes or the endoplasmic reticulum requires adenosine 5′-triphosphate–dependent pumps and is energetically costly. Therefore, massive global Ca^{2+} bursts are unlikely to occur very frequently, in contrast to the common involvement of Ca^{2+} ions in local cell functions. Despite this distinctive nature, the question which physiological immune cell functions cause or require Ca^{2+} bursts remains unanswered and merits closer attention. It is reasonable to assume that the underlying physiological events occur only occasionally and tend to engage the whole cell. Given the prominence and easy detectability of Ca^{2+} bursts, a better understanding of the underlying events could provide a valuable foundation for new insights and tools in biomedical research and clinical diagnostics.

A closer look at the cause-and-effect sequences or mechanisms governing Ca^{2+} bursts in motile immune cells benefits greatly from a reductionist approach that separates recognition of chemotactic cues from other elements of chemotactic cell migration such as cell-substrate adhesion. Unlike other chemotaxis assays, our single-live-cell, pure-chemotaxis experiments were designed for this purpose. As a consequence, we were able to establish that complement-mediated, pure chemotaxis neither requires nor causes Ca^{2+} bursts, consistent with previous studies that used formyl peptides to stimulate chemotaxis of adherent neutrophils (32, 33). In as much as chemoattractant gradient sensing and pseudopod

formation can be viewed as local processes, our result agrees well with the assumption that Ca^{2+} bursts are linked to global cellular events.

Having ruled out that the ligation of GPCRs of anaphylatoxins acts as a direct biochemical cause of Ca^{2+} bursts under physiological conditions, we pursued two lines of further inquiry. First, we forced the occurrence of Ca^{2+} bursts in nonadherent neutrophils by subjecting the cells to jets of solutions containing supraphysiological concentrations of C5a. Second, we examined mechanical aspects of the cell behavior during pure chemotaxis. Although our jet experiments revealed important qualitative insights, their quantitative interpretation is difficult. Ever-present pressure drifts in the open experiment chamber make it impossible to completely stop flow through the C5a pipette over an appreciable amount of time. To avoid contamination of the chamber, we therefore maintained a slightly negative pressure in the C5a pipette between actual single-cell tests. As a consequence, the exact moment when, after pressure reversal, the ejected jet started delivering C5a was unknown. Furthermore, neither the concentration of C5a reaching the front of the cell nor its gradient along the cell surface was accurately known, for the following reasons. First, carboxypeptidases in the supplied donor serum rapidly metabolize C5a (37). Second, the flow rate at which the C5a solution is expelled from the pipette tip is difficult to assess because it depends on the pipette geometry and possible additional flow bottle-necks in the pressure system. Third, the flow profile of the jet is affected by nearby walls and the changing cell shape. In addition to these uncertainties regarding the biochemical stimulation of the cells, it is also important to bear in mind that human neutrophils can sense and be activated by fluidic shear flow alone (7–10, 59–61).

Our jet experiments identified two causal stimuli of Ca^{2+} bursts in nonadherent neutrophils: (i) costimulation of the cells by a combination of fluid shear flow and moderate C5a concentrations (typically on the order of 1 to 100 nM) and (ii) high C5a concentrations alone (on the order of 0.1 μM or more). These observations are qualitatively consistent with the behavior of adherent neutrophils, which have been shown to be able to sense shear flow (59–61) and to exhibit Ca^{2+} bursts in response to a combination of shear flow and the chemoattractants interleukin-8 (7) or fMLP (8). Moreover, adherent human neutrophils are able to chemotax without Ca^{2+} bursts when stimulated by low concentrations of fMLP, whereas high fMLP concentrations triggered Ca^{2+} bursts and stopped chemotaxis (33). In the latter study, the neutrophils might also have been co-stimulated by shear flow. Note that the similarities between previously published studies and our findings exist despite the use of different chemoattractants. In general, one may not take for granted that different chemoattractants elicit a common neutrophil response. Different chemoattractants can activate distinct—and even mutually inhibitory—signaling processes in the same cell (49, 50). Moreover, the quantitative interpretation of similarities between adherent and nonadherent cells is problematic because most types of adhesion to a substrate or phagocytic target cause activation of immune cells. For example, the release of reactive oxygen intermediates can vary up to 100-fold between adherent and nonadherent neutrophils under otherwise identical conditions (62).

As part of our second line of inquiry, we carefully examined the cell morphology during pure chemotaxis under near-physiological conditions where no Ca^{2+} bursts occurred. By

quantifying the degree of cell deformation in terms of the increase of the apparent cell surface area, we discovered a large (about eightfold) difference between the increase in surface area due to purely chemotactic deformations and the enormous capacity of these cells to change their shape during adhesion-dependent processes such as phagocytosis or migration. Perhaps the most interesting outcome of this quantitative assessment was the coincidence between the maximum surface area expansion measured during pure chemotaxis (30%) and the amount of cortical slack that neutrophils are known to have (57). This result implies that the largest protrusive forces that nonadherent neutrophils can generate are much lower than the forces that adherent neutrophils are able to produce (36).

Together, these experiments expose two seemingly contradictory mechanical correlates of Ca^{2+} bursts. The limited extent of protrusion in the absence of Ca^{2+} bursts (Fig. 5) implies that such bursts might be a prerequisite for larger protrusive deformations. By contrast, when Ca^{2+} bursts did occur in our jet experiments, the accompanying cell deformation opposed protrusion (Figs. 3, B and C, and 4 and fig. S3), although it is important to bear in mind that the high concentrations of C5a required to trigger Ca^{2+} bursts in nonadherent neutrophils are unlikely to be encountered in vivo. A quantitative analysis of C5a production under near-physiological conditions showed that the highest concentrations of C5a are found in the immediate vicinity of pathogenic particles (37). On the other hand, this analysis also showed that the C5a concentration correlates positively with the particle size. Therefore, the concentrations of both C5a and the derived C5a(desArg) are expected to rise during infections. C5a(desArg) binds to the C5a receptor with a lower affinity than C5a, but high concentrations of C5a(desArg) still significantly contribute to immune cell activation (63). It is therefore possible that, in pathological situations, the total concentration of C5a and C5a(desArg) reaches values high enough to stall chemotaxis by the same mechanism that causes the contractile cell deformation reported here. High C5a concentrations are an important factor in the neutrophil paralysis that is observed in sepsis (40–44). Thus, the type of single-cell experiments presented here could provide an instructive window into the behavior of immune cells during sepsis and other pathological conditions.

Both tangential and normal (perpendicular) surface forces are responsible for the peculiar cell deformation that accompanies Ca^{2+} bursts in nonadherent neutrophils. If we conceptually translate these forces to neutrophils that adhere to a substrate or phagocytic target under physiological conditions, then their actual role becomes clearer. As part of a “push-and-lock” mechanism (36), the normal force stabilizes adhesion by flattening the cell against the substrate or particle (23), thus locally counteracting protrusive forces that would otherwise lift the cell off the substrate or push phagocytic targets away. The tangential force, or cortical tension, acts globally to pull phagocytic particles into the cell (36) or to reel in the trailing end of a cell crawling on a substrate. Our results (Figs. 3, B and C, and 4) suggest that exposure of neutrophils to excess C5a causes a mechanical imbalance that boosts the contractile forces beyond the ability of protrusive forces to keep pace.

Central to the balance between contraction and protrusion are cytoskeletal membrane anchors, which are structural linkages that connect the cytoplasmic domains of transmembrane receptors to the actin cytoskeleton either directly or through adapter proteins (34, 36, 64). The function of many of these linkages involves Ca^{2+}. Examples include the

cleavage of anchor components by proteases like calpain (65–68), the interaction of β2-integrins with Ca^{2+} channels (7–9, 11, 27, 28), and the involvement of moesin in P-selectin glycoprotein ligand-1–mediated Ca^{2+} signaling (10). Complement receptor 3 (CR3; also known as Mac-1, CD11b/CD18, and $\alpha_M\beta_2$ integrin) seems particularly suited to function as a mechanistic switchboard in the regulation of Ca^{2+}-related neutrophil deformations (11, 27, 28). CR3 is one of the most promiscuous immune cell receptors (69, 70), capable of funneling a multitude of stimuli into one or a few common response pipelines. Not only does the affinity of CR3 depend on divalent cations, but it can also be adjusted by conformational changes induced by extracellular and intracellular stimuli, including the exposure to C5a and the ligation of other phagocytic receptors (71). The number of CR3 molecules on the surface of neutrophils can be increased up to threefold through exposure to chemokines like fMLP (72) and C5a (73). Last, neutrophils are able to regulate the mobility of CR3 (29, 71, 74), implying that the cells can control the state of the receptor's cytoskeletal anchor. The sum of these features tentatively assigns to structural linkages involving CR3, its sibling lymphocyte function-associated antigen–1, or similar receptors—along with their cytoskeletal anchors—a pivotal mechanistic role in the governance of Ca^{2+} bursts in immune cells.

In summary, pure chemotactic protrusion under physiological conditions is characterized by the absence of Ca^{2+} bursts, cell adhesion, and surface area increases beyond the extent permitted by the inherent slack of the neutrophil surface. It is possible that the release of cytoskeletal membrane anchors locally eases the formation of protrusive pseudopods, but this type of assist does not require Ca^{2+} bursts during pure chemotaxis. A qualitatively different mode of cytoskeletal organization and dynamics governs the balance of protrusion and contraction during larger deformations of adherent neutrophils. Maintenance of this balance across various immune cell functions requires the expedient coordination of locking or release of cytoskeletal membrane anchors. We hypothesize that the mechanistic switch between the two modes of cytoskeletal behavior is an adhesion-dependent, global event that is mediated by a Ca^{2+} burst. This hypothesis is consistent with previous interdisciplinary studies of Ca^{2+} bursts in neutrophils (7–10, 23, 29, 33) and agrees well with the established behavior of the cortical tension of these cells (57). It assigns to Ca^{2+} bursts a primarily mechanotransductory function. Although further dissection of the nature of this mechanistic switch is beyond this study's focus on pure chemotaxis, our findings have taken us closer to a sound understanding of the physiological role of Ca^{2+} bursts in immune cells.

MATERIALS AND METHODS

Human neutrophil isolation

Written informed consent was obtained from all subjects. The Institutional Review Board of the University of California, Davis approved the protocol for this study. Neutrophils were isolated from whole blood of healthy donors by immunomagnetic negative selection using the EasySep Direct Human Neutrophil Isolation Kit (STEMCELL Technologies). First, 25 μl each of the isolation cocktail and the magnetic bead solution were added to a small volume of blood (~0.5 ml) to facilitate cross-linking of cells other than neutrophils to magnetic beads using tetrameric antibody complexes. After 5 min, the sample was diluted with phosphate-buffered saline (PBS; IBI Scientific) containing 2% fetal bovine serum and 1

mM EDTA (EasySep Buffer, STEMCELL Technologies) at a minimum 2:1 ratio and placed adjacent to a magnet. After 10 min, 0.5 to 1.0 ml of the enriched, lighter-colored neutrophil fraction was carefully transferred into a new test tube, and another 25 μl of the magnetic bead solution was added. After two more 5-min magnetic separation cycles, the cells were resuspended in Hanks' balanced salt solution (HBSS) containing 1.26 mM Ca^{2+} and 0.9 mM Mg^{2+} (HBSS with Ca^{2+} and Mg^{2+}; Thermo Fisher Scientific) and treated with Fluo-4, as described below.

Fluo-4 labeling of live human neutrophils and reduction of side effects

Fluo-4 (Fluo-4, AM; Thermo Fisher Scientific) was reconstituted in anhydrous dimethyl sulfoxide (Thermo Fisher Scientific) at a concentration of 1 mM and stored at 4°C protected from light. For each experiment, 1 ml of isolated neutrophil suspension was incubated with 0.5 μl of Fluo-4 solution at 37°C for 25 min and then resuspended in HBSS. The labeled cells were gently rotated in a dark container at room temperature until use.

We encountered the following side effects of the fluorescent Ca^{2+} dye Fluo-4. When examining neutrophils preloaded with Fluo-4 under the high-power excitation light provided by a mercury arc lamp, we occasionally observed spontaneous increases of the intensity of the emitted fluorescence without any other sign of neutrophil activation, presumably due to photo or heat activation of the dye. Such false-positives were overcome by using, as our standard excitation source, the cyan light-emitting diode (LED) of a SPECTRA X light engine (Lumencor), strobed at 0.5-s intervals at 10% of its maximum intensity and filtered through an ET480/40x bandpass excitation filter (Chroma Technology). Despite this low-power excitation, we still frequently observed cell death toward the end of an experiment, usually after a Ca^{2+} burst. This cytotoxic effect of Fluo-4 was notice-ably reduced after we decreased the concentration of the dye in the neutrophil-preincubation buffer to half the recommended value. Even then, we found that the cortical tension of the neutrophils was often slightly increased, causing the cells to appear stiffer than in the absence of Fluo-4. Therefore, we cannot exclude that the presence of Fluo-4 affected the values of our quantitative measurements to some extent. However, throughout the relevant stages of our experiments (pure chemotaxis, adhesion, and phagocytosis), the time-dependent behavior of neutrophils preloaded with Fluo-4 was the same as in numerous previous experiments without the dye. Therefore, it seems reasonable to assume that Fluo-4 did not qualitatively affect the main results reported here.

Preparation of target particles

Zymosan particles (Sigma-Aldrich) were suspended in PBS at 3 to 10 mg/ml, boiled in a water bath for 30 min, washed twice in PBS, and stored at 4°C. On each day of experimentation, the solution was sonicated for 30 to 60 min before use. Whole 1,3/1,6-β-glucan particles (WGP Dispersible, InvivoGen) were suspended in PBS at 2 to 10 mg/ml. After three washes in PBS, the solution was sonicated for 30 to 60 min. The solution was stored at 4°C. Sonication was repeated on each day of experimentation. Polystyrene microspheres were opsonized with antibody as described previously (57). In short, beads with 5.0- or 9.7-μm nominal diameter (Duke Standards Microspheres, Thermo Fisher Scientific) were incubated overnight at 4°C in PBS containing bovine serum albumin (BSA;

10 mg/ml; AMRESCO). After three washes in PBS with 0.01% Tween 20 (MilliporeSigma), the beads were incubated with rabbit polyclonal anti-bovine albumin antibody (Thermo Fisher Scientific) at room temperature for 1 hour. The beads were then washed three more times in the PBS/Tween solution and resuspended in PBS for storage at 4°C.

Single-live-cell, single-target experiments

An inverted microscope (Zeiss) was equipped with a dual micropipette manipulation system, as described previously (58, 75). The experiment chamber was filled with HBSS with Ca^{2+} and Mg^{2+}. For experiments with zymosan or β-glucan particles, the buffer was supplemented with 20% autologous donor serum. When using opsonized microspheres, the buffer was supplemented with serum or BSA (20 mg/ml). All experiments using human neutrophils were performed at room temperature.

Jet experiments

Native (not recombinant) human C5a (Complement Technology Inc.) was diluted in serum-free buffer to the desired concentration and preloaded into the pipette facing the cells. To minimize contamination of the experiment chamber, we kept the C5a pipette under a slight suction (negative) pressure until the start of each single-cell test. Once the cell-holding pipette and the C5a pipette had been positioned at the desired distance from one another, the pressure in the C5a pipette was reversed to the desired positive value, causing its solution to be expelled in a jet directed toward the cell.

Dual-camera setup for simultaneous recording of fluorescence and bright-field images

Micropipette manipulation requires a low-noise environment. To prevent vibrations caused by mechanical shutters or filter wheels, we used a dual-camera setup that allowed us to record fluorescence and bright-field images without such devices (fig. S1). The microscope was coupled to two video cameras using a Zeiss dual-camera adapter. A uEye USB-3 camera (UI-3240, 1stVision Inc.) was used to record bright-field images, and a sensitive electron-multiplying CCD camera (Andor iXon Ultra, Technical Instruments) was synchronized with an electronically strobed LED (SPECTRA X light engine) and used to record fluorescence images under low-intensity excitation. White LED light (Thorlabs) was filtered to produce red light for bright-field illumination. Epi-illumination by the cyan LED of the SPECTRA X light engine provided optimum excitation of Fluo-4. The emitted green light was passed through suitable dichroic mirrors and an emission filter (fig. S1) to be imaged by the EMCCD camera.

Measurement of the cell surface area

The principal workflow of our measurement of the cell surface area involved the following steps (fig. S4). First, we manually traced the boundary of the cell body outside the pipette in a suitable video image (fig. S4). We then found the mathematical expression of a Fourier-smoothed, continuous representation of the resulting polygon (fig. S4). The 2D region enclosed by this curve was assumed to be the cross section of a rotationally symmetric 3D body containing the symmetry axis. We also assumed that the axis of rotation ran through the 2D center of mass of the cross-sectional region. We next determined those two straight

lines containing the mass center for which the contour parts on either side exhibited maximal mirror symmetry. From these two candidates, we chose the most likely axis of rotation based on the experimental context, usually defined by the position of the nearby target particle. The two parts of the contour on either side of this axis were not usually exact mirror-symmetric replicas of each other, so we approximated the actual contour with a mirror-symmetric version, which here is the average of the two parts. Finally, we used this symmetric contour to generate a 3D image of the resulting axisymmetric shape (fig. S4). We used a slightly different approach in our surface area calculation. Rather than averaging the two contour parts, we generated separate axisymmetric 3D bodies for each of them and then calculated the average of the surface areas of these two bodies.

As long as the osmotic conditions do not change, the cell volume remains constant during the deformations considered here. We calculated the total volume of the deformed cell as the sum of the volume of the axisymmetric approximation of the cell body outside the pipette and the volume of the cell projection in the pipette, which was assumed to consist of cylindrical and hemispherical parts. If this total volume was different from the volume of the same cell measured in its initially relaxed, spherical state, then we enforced the volume constraint by rescaling the outer cell body. Only then did we calculate the total surface of the deformed cell. Our calculation accounted for the hole in the surface of the outer cell body at the pipette entrance by subtracting the area of a disc that had the same radius as the pipette.

Supplementary Material

Refer to Web version on PubMed Central for supplementary material.

Funding:

This work was supported by the NIH (grant R01 GM098060).

REFERENCES AND NOTES

1. White JR, Naccache PH, Molski TFP, Borgeat P, Sha'afi RI, Direct demonstration of increased intracellular concentration of free calcium in rabbit and human neutrophils following stimulation by chemotactic factor. Biochem. Biophys. Res. Commun 113, 44–50 (1983). [PubMed: 6305358]
2. Lew DP, Receptor signalling and intracellular calcium in neutrophil activation. Eur. J. Clin. Invest 19, 338–346 (1989). [PubMed: 2550240]
3. Norgauer J, Dobos G, Kownatzki E, Dahinden C, Burger R, Kupper R, Gierschik P, Complement fragment C3a stimulates Ca^{2+} influx in neutrophils via a pertussis-toxin-sensitive G protein. Eur. J. Biochem 217, 289–294 (1993). [PubMed: 8223566]
4. Schorr W, Swandulla D, Zeilhofer HU, Mechanisms of IL-8-induced Ca^{2+} signaling in human neutrophil granulocytes. Eur. J. Immunol 29, 897–904 (1999). [PubMed: 10092093]
5. Ibrahim FB, Pang SJ, Melendez AJ, Anaphylatoxin signaling in human neutrophils. A key role for sphingosine kinase. J. Biol. Chem 279, 44802–44811 (2004). [PubMed: 15302883]
6. Partida-Sánchez S, Iribarren P, Moreno-García ME, Gao J-L, Murphy PM, Oppenheimer N, Wang JM, Lund FE, Chemotaxis and calcium responses of phagocytes to formyl peptide receptor ligands is differentially regulated by cyclic ADP ribose. J. Immunol 172, 1896–1906 (2004). [PubMed: 14734775]
7. Schaff UY, Yamayoshi I, Tse T, Griffin D, Kibathi L, Simon SI, Calcium flux in neutrophils synchronizes β_2 integrin adhesive and signaling events that guide inflammatory recruitment. Ann. Biomed. Eng 36, 632–646 (2008). [PubMed: 18278555]

8. Schaff UY, Dixit N, Procyk E, Yamayoshi I, Tse T, Simon SI, Orai1 regulates intracellular calcium, arrest, and shape polarization during neutrophil recruitment in shear flow. Blood 115, 657–666 (2010). [PubMed: 19965684]
9. Dixit N, Yamayoshi I, Nazarian A, Simon SI, Migrational guidance of neutrophils is mechanotransduced via high-affinity LFA-1 and calcium flux. J. Immunol 187, 472–481 (2011). [PubMed: 21632714]
10. Huang B, Ling Y, Lin J, Du X, Fang Y, Wu J, Force-dependent calcium signaling and its pathway of human neutrophils on P-selectin in flow. Protein Cell 8, 103–113 (2017). [PubMed: 28097631]
11. Jaconi ME, Theler JM, Schlegel W, Appel RD, Wright SD, Lew PD, Multiple elevations of cytosolic-free Ca^{2+} in human neutrophils: Initiation by adherence receptors of the integrin family. J. Cell Biol 112, 1249–1257 (1991). [PubMed: 1900302]
12. Clapham DE, Calcium signaling. Cell 80, 259–268 (1995). [PubMed: 7834745]
13. Feske S, ORAI1 and STIM1 deficiency in human and mice: Roles of store-operated Ca^{2+} entry in the immune system and beyond. Immunol. Rev 231, 189–209 (2009). [PubMed: 19754898]
14. Bogeski I, Kummerow C, Al-Ansary D, Schwarz EC, Koehler R, Kozai D, Takahashi N, Peinelt C, Griesemer D, Bozem M, Mori Y, Hoth M, Niemeyer BA, Differential redox regulation of ORAI ion channels: A mechanism to tune cellular calcium signaling. Sci. Signal 3, ra24 (2010). [PubMed: 20354224]
15. Clemens RA, Lowell CA, Store-operated calcium signaling in neutrophils. J. Leukoc. Biol 98, 497–502 (2015). [PubMed: 25714804]
16. Sogkas G, Vögtle T, Rau E, Gewecke B, Stegner D, Schmidt RE, Nieswandt B, Gessner JE, Orai1 controls C5a-induced neutrophil recruitment in inflammation. Eur. J. Immunol 45, 2143–2153 (2015). [PubMed: 25912155]
17. Saul S, Gibhardt CS, Schmidt B, Lis A, Pasieka B, Conrad D, Jung P, Gaupp R, Wonnenberg B, Diler E, Stanisz H, Vogt T, Schwarz EC, Bischoff M, Herrmann M, Tschernig T, Kappl R, Rieger H, Niemeyer BA, Bogeski I, A calcium-redox feedback loop controls human monocyte immune responses: The role of ORAI Ca^{2+} channels. Sci. Signal 9, ra26 (2016). [PubMed: 26956485]
18. Demaurex N, Nunes P, The role of STIM and ORAI proteins in phagocytic immune cells. Am. J. Physiol. Cell Physiol 310, C496–C508 (2016). [PubMed: 26764049]
19. Zimmerli W, Reber AM, Dahinden CA, The role of formylpeptide receptors, C5a receptors, and cytosolic-free calcium in neutrophil priming. J. Infect. Dis 161, 242–249 (1990). [PubMed: 2153739]
20. Elsner J, Kaever V, Emmendörffer A, Breidenbach T, Lohmann-Matthes M-L, Roesler J, Heterogeneity in the mobilization of cytoplasmic calcium by human polymorphonuclear leukocytes in response to fMLP, C5a and IL-8/NAP-1. J. Leukoc. Biol 51, 77–83 (1992). [PubMed: 1740648]
21. Partida-Sánchez S, Cockayne DA, Monard S, Jacobson EL, Oppenheimer N, Garvy B, Kusser K, Goodrich S, Howard M, Harmsen A, Randall TD, Lund FE, Cyclic ADP-ribose production by CD38 regulates intracellular calcium release, extracellular calcium influx and chemotaxis in neutrophils and is required for bacterial clearance in vivo. Nat. Med 7, 1209–1216 (2001). [PubMed: 11689885]
22. Itagaki K, Kannan KB, Livingston DH, Deitch EA, Fekete Z, Hauser CJ, Store-operated calcium entry in human neutrophils reflects multiple contributions from independently regulated pathways. J. Immunol 168, 4063–4069 (2002). [PubMed: 11937565]
23. Beste MT, Lomakina EB, Hammer DA, Waugh RE, Immobilized IL-8 triggers phagocytosis and dynamic changes in membrane microtopology in human neutrophils. Ann. Biomed. Eng 43, 2207–2219 (2015). [PubMed: 25582838]
24. Jaconi ME, Lew DP, Carpentier JL, Magnusson KE, Sjögren M, Stendahl O, Cytosolic free calcium elevation mediates the phagosome-lysosome fusion during phagocytosis in human neutrophils. J. Cell Biol 110, 1555–1564 (1990). [PubMed: 2110568]
25. Marks PW, Maxfield FR, Local and global changes in cytosolic free calcium in neutrophils during chemotaxis and phagocytosis. Cell Calcium 11, 181–190 (1990). [PubMed: 2354498]

26. Theler JM, Lew DP, Jaconi ME, Krause KH, Wollheim CB, Schlegel W, Intracellular pattern of cytosolic Ca2+ changes during adhesion and multiple phagocytosis in human neutrophils. Dynamics of intracellular Ca2+ stores. Blood 85, 2194–2201 (1995). [PubMed: 7718891]
27. Pettit EJ, Hallett MB, Pulsatile Ca^{2+} influx in human neutrophils undergoing CD11b/CD18 integrin engagement. Biochem. Biophys. Res. Commun 230, 258–261 (1997). [PubMed: 9016761]
28. Löfgren R, Serrander L, Forsberg M, Wilsson Å, Wasteson Å, Stendahl O, CR3, FcγRIIA and FcγRIIIB induce activation of the respiratory burst in human neutrophils: The role of intracellular Ca^{2+}, phospholipase D and tyrosine phosphorylation. Biochim. Biophys. Acta 1452, 46–59 (1999). [PubMed: 10525159]
29. Dewitt S, Hallett MB, Cytosolic free Ca^{2+} changes and calpain activation are required for β integrin–accelerated phagocytosis by human neutrophils. J. Cell Biol 159, 181–189 (2002). [PubMed: 12379807]
30. Nunes P, Demaurex N, The role of calcium signaling in phagocytosis. J. Leukoc. Biol 88, 57–68 (2010). [PubMed: 20400677]
31. Marks PW, Maxfield FR, Transient increases in cytosolic free calcium appear to be required for the migration of adherent human neutrophils. J. Cell Biol 110, 43–52 (1990). [PubMed: 2295684]
32. Meshulam T, Proto P, Diamond RD, Melnick DA, Calcium modulation and chemotactic response: Divergent stimulation of neutrophil chemotaxis and cytosolic calcium response by the chemotactic peptide receptor. J. Immunol 137, 1954–1960 (1986). [PubMed: 3745918]
33. Laffafian I, Hallett MB, Does cytosolic free Ca2+ signal neutrophil chemotaxis in response to formylated chemotactic peptide? J. Cell Sci 108, (Pt 10) 3199–3205 (1995). [PubMed: 7593281]
34. Heinrich V, Lee C-Y, Blurred line between chemotactic chase and phagocytic consumption: An immunophysical single-cell perspective. J. Cell Sci 124, 3041–3051 (2011). [PubMed: 21914817]
35. Mankovich AR, Lee C-Y, Heinrich V, Differential effects of serum heat treatment on chemotaxis and phagocytosis by human neutrophils. PLOS ONE 8, e54735 (2013). [PubMed: 23349959]
36. Heinrich V, Controlled one-on-one encounters between immune cells and microbes reveal mechanisms of phagocytosis. Biophys. J 109, 469–476 (2015). [PubMed: 26244729]
37. Heinrich V, Simpson III WD, Francis EA, Analytical prediction of the spatiotemporal distribution of chemoattractants around their source: Theory and application to complement-mediated chemotaxis. Front. Immunol 8, 578 (2017). [PubMed: 28603522]
38. Merle NS, Church SE, Fremeaux-Bacchi V, Roumenina LT, Complement system part I—Molecular mechanisms of activation and regulation. Front. Immunol 6, 262 (2015). [PubMed: 26082779]
39. Guo R-F, Ward PA, Role of C5a in inflammatory responses. Annu. Rev. Immunol 23, 821–852 (2005). [PubMed: 15771587]
40. Huber-Lang MS, Younkin EM, Sarma JV, McGuire SR, Lu KT, Guo RF, Padgaonkar VA, Curnutte JT, Erickson R, Ward PA, Complement-induced impairment of innate immunity during sepsis. J. Immunol 169, 3223–3231 (2002). [PubMed: 12218141]
41. Ward PA, The dark side of C5a in sepsis. Nat. Rev. Immunol 4, 133–142 (2004). [PubMed: 15040586]
42. Zhang F, Liu A-L, Gao S, Ma S, Guo SB, Neutrophil dysfunction in sepsis. Chin Med J (Engl) 129, 2741–2744 (2016). [PubMed: 27824008]
43. Bhan C, Dipankar P, Chakraborty P, Sarangi PP, Role of cellular events in the pathophysiology of sepsis. Inflamm. Res 65, 853–868 (2016). [PubMed: 27392441]
44. Shen X-F, Cao K, Jiang J.-p., Guan W-X, Du J-F, Neutrophil dysregulation during sepsis: An overview and update. J. Cell. Mol. Med 21, 1687–1697 (2017). [PubMed: 28244690]
45. Marc MM, Kristan SS, Rozman A, Kern I, Flezar M, Kosnik M, Korosec P, Complement factor C5a in acute exacerbation of Chronic Obstructive Pulmonary Disease. Scand. J. Immunol 71, 386–391 (2010). [PubMed: 20500690]
46. Stöve S, Welte T, Wagner TO, Kola A, Klos A, Bautsch W, Köhl J, Circulating complement proteins in patients with sepsis or systemic inflammatory response syndrome. Clin. Diagn. Lab. Immunol 3, 175–183 (1996). [PubMed: 8991632]

47. Lechner J, Chen M, Hogg RE, Toth L, Silvestri G, Chakravarthy U, Xu H, Higher plasma levels of complement C3a, C4a and C5a increase the risk of subretinal fibrosis in neovascular age-related macular degeneration: Complement activation in AMD. Immun. Aeging 13, 4 (2016).
48. Francis EA, Heinrich V, Quantifying the sensitivity of human immune cells to chemoattractant. Biophys. J 112, 834–837 (2017). [PubMed: 28185642]
49. Heit B, Tavener S, Raharjo E, Kubes P, An intracellular signaling hierarchy determines direction of migration in opposing chemotactic gradients. J. Cell Biol 159, 91–102 (2002). [PubMed: 12370241]
50. Heit B, Robbins SM, Downey CM, Guan Z, Colarusso P, Miller BJ, Jirik FR, Kubes P, PTEN functions to 'prioritize' chemotactic cues and prevent 'distraction' in migrating neutrophils. Nat. Immunol 9, 743–752 (2008). [PubMed: 18536720]
51. Lee C-Y, Thompson GR III, Hastey CJ, Hodge GC, Lunetta JM, Pappagianis D, Heinrich V, *Coccidioides* endospores and spherules draw strong chemotactic, adhesive, and phagocytic responses by individual human neutrophils. PLOS ONE 10, e0129522 (2015). [PubMed: 26070210]
52. Wangdi T, Lee C-Y, Spees AM, Yu C, Kingsbury DD, Winter SE, Hastey CJ, Wilson RP, Heinrich V, Bäumler AJ, The Vi capsular polysaccharide enables *Salmonella enterica* serovar typhi to evade microbe-guided neutrophil chemotaxis. PLOS Pathog. 10, e1004306 (2014). [PubMed: 25101794]
53. Chodniewicz D, Alteraifi AM, Zhelev DV, Experimental evidence for the limiting role of enzymatic reactions in chemoattractant-induced pseudopod extension in human neutrophils. J. Biol. Chem 279, 24460–24466 (2004). [PubMed: 15051729]
54. Zhelev DV, Alteraifi AM, Chodniewicz D, Controlled pseudopod extension of human neutrophils stimulated with different chemoattractants. Biophys. J 87, 688–695 (2004). [PubMed: 15240502]
55. Ting-Beall HP, Needham D, Hochmuth RM, Volume and osmotic properties of human neutrophils. Blood 81, 2774–2780 (1993). [PubMed: 8490184]
56. Herant M, Heinrich V, Dembo M, Mechanics of neutrophil phagocytosis: Experiments and quantitative models. J. Cell Sci 119, 1903–1913 (2006). [PubMed: 16636075]
57. Herant M, Heinrich V, Dembo M, Mechanics of neutrophil phagocytosis: Behavior of the cortical tension. J. Cell Sci 118, 1789–1797 (2005). [PubMed: 15827090]
58. Lee C-Y, Herant M, Heinrich V, Target-specific mechanics of phagocytosis: Protrusive neutrophil response to zymosan differs from the uptake of antibody-tagged pathogens. J. Cell Sci 124, 1106–1114 (2011). [PubMed: 21385838]
59. Makino A, Prossnitz ER, Bünemann M, Wang JM, Yao W, Schmid-Schönbein GW, G protein-coupled receptors serve as mechanosensors for fluid shear stress in neutrophils. Am. J. Physiol. Cell Physiol 290, C1633–C1639 (2006). [PubMed: 16436471]
60. Mitchell MJ, King MR, Shear-induced resistance to neutrophil activation via the formyl peptide receptor. Biophys. J 102, 1804–1814 (2012). [PubMed: 22768936]
61. Mitchell MJ, Lin KS, King MR, Fluid shear stress increases neutrophil activation via platelet-activating factor. Biophys. J 106, 2243–2253 (2014). [PubMed: 24853753]
62. Nathan CF, Neutrophil activation on biological surfaces. Massive secretion of hydrogen peroxide in response to products of macrophages and lymphocytes. J. Clin. Invest 80, 1550–1560 (1987). [PubMed: 2445780]
63. Reis ES, Chen H, Sfyroera G, Monk PN, Köhl J, Ricklin D, Lambris JD, C5a receptor-dependent cell activation by physiological concentrations of desarginated C5a: Insights from a novel label-free cellular assay. J. Immunol 189, 4797–4805 (2012). [PubMed: 23041570]
64. Herant M, Lee C-Y, Dembo M, Heinrich V, Protrusive push versus enveloping embrace: Computational model of phagocytosis predicts key regulatory role of cytoskeletal membrane anchors. PLOS Comput. Biol 7, e1001068 (2011). [PubMed: 21298079]
65. Franco S, Perrin B, Huttenlocher A, Isoform specific function of calpain 2 in regulating membrane protrusion. Exp. Cell Res 299, 179–187 (2004). [PubMed: 15302585]
66. Franco SJ, Rodgers MA, Perrin BJ, Han J, Bennin DA, Critchley DR, Huttenlocher A, Calpain-mediated proteolysis of talin regulates adhesion dynamics. Nat. Cell Biol 6, 977–983 (2004). [PubMed: 15448700]

67. Cortesio CL, Boateng LR, Piazza TM, Bennin DA, Huttenlocher A, Calpain-mediated proteolysis of paxillin negatively regulates focal adhesion dynamics and cell migration. J. Biol. Chem 286, 9998–10006 (2011). [PubMed: 21270128]

68. Dewitt S, Francis RJ, Hallett MB, Ca^{2+} and calpain control membrane expansion during the rapid cell spreading of neutrophils. J. Cell Sci 126, 4627–4635 (2013). [PubMed: 23943875]

69. Diamond MS, Garcia-Aguilar J, Bickford JK, Corbi AL, Springer TA, The I domain is a major recognition site on the leukocyte integrin Mac-1 (CD11b/CD18) for four distinct adhesion ligands. J. Cell Biol 120, 1031–1043 (1993). [PubMed: 7679388]

70. Podolnikova NP, Podolnikov AV, Haas TA, Lishko VK, Ugarova TP, Ligand recognition specificity of leukocyte integrin αMβ2 (Mac-1, CD11b/CD18) and its functional consequences. Biochemistry 54, 1408–1420 (2015). [PubMed: 25613106]

71. Jongstra-Bilen J, Harrison R, Grinstein S, Fcγ-receptors induce Mac-1 (CD11b/CD18) mobilization and accumulation in the phagocytic cup for optimal phagocytosis. J. Biol. Chem 278, 45720–45729 (2003). [PubMed: 12941957]

72. Lomakina E, Knauf PA, Schultz JB, Law F-Y, McGraw MD, Waugh RE, Activation of human neutrophil Mac-1 by anion substitution. Blood Cells Mol. Dis 42, 177–184 (2009). [PubMed: 19246218]

73. Hünniger K, Bieber K, Martin R, Lehnert T, Figge MT, Löffler J, Guo RF, Riedemann NC, Kurzai O, A second stimulus required for enhanced antifungal activity of human neutrophils in blood is provided by anaphylatoxin C5a. J. Immunol 194, 1199–1210 (2015). [PubMed: 25539819]

74. Graham IL, Gresham HD, Brown EJ, An immobile subset of plasma-membrane Cd11b/Cd18 (Mac-1) is involved in phagocytosis of targets recognized by multiple receptors. J. Immunol 142, 2352–2358 (1989). [PubMed: 2538507]

75. Heinrich V, Rawicz W, Automated, high-resolution micropipet aspiration reveals new insight into the physical properties of fluid membranes. Langmuir 21, 1962–1971 (2005). [PubMed: 15723496]

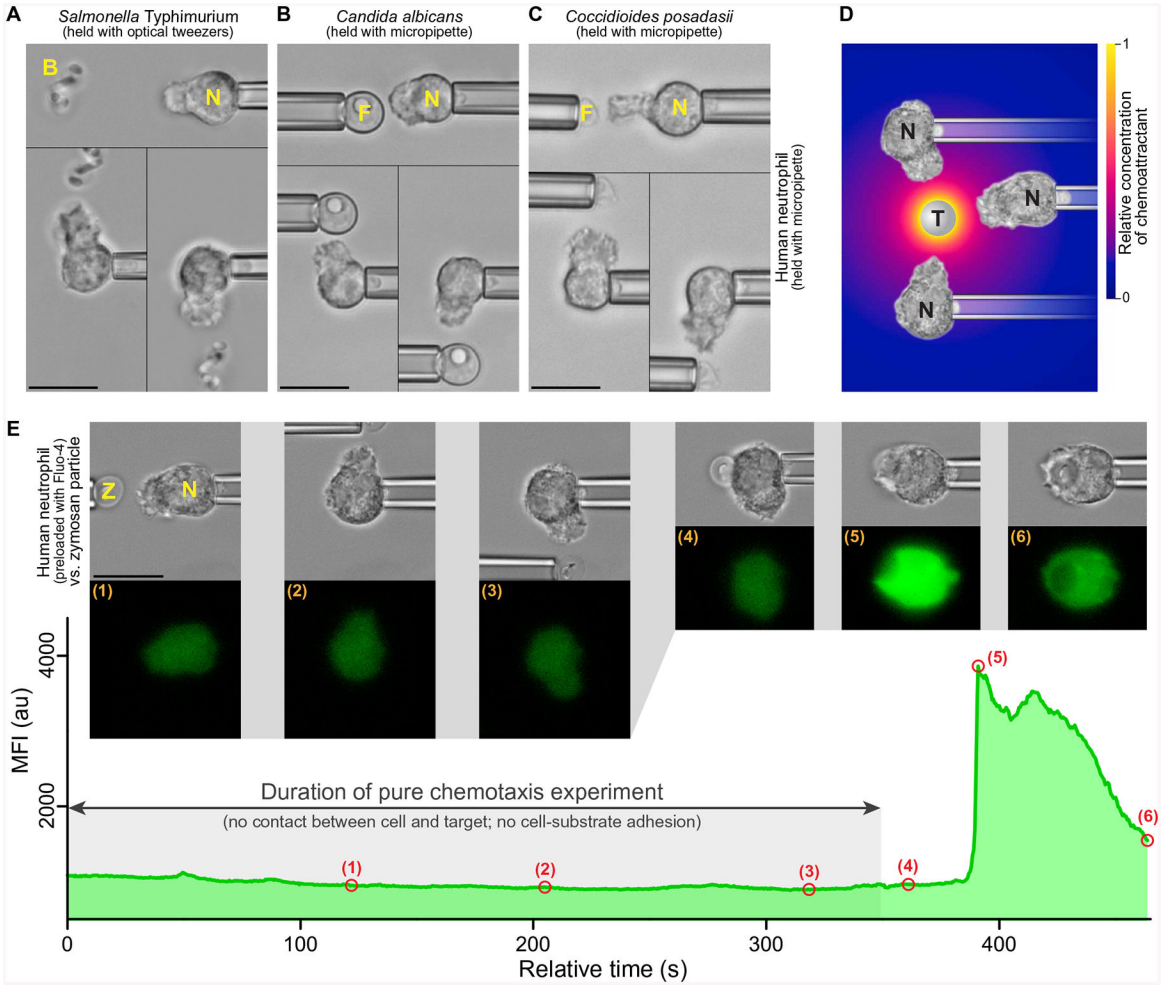

Fig. 1. Complement-mediated, pure chemotaxis, and Ca^{2+} bursts.

(**A** to **C**) Examples of single-live-cell, pure-chemotaxis experiments (51, 52) in which human neutrophils (N) were placed near bacterial (B) or fungal (F) pathogens. The nonadherent neutrophils were held with gentle suction pressure at the tip of a micropipette and placed near a cluster of *S.* Typhimurium bacteria trapped with optical tweezers (A), a single *C. albicans* cell held with a micropipette (B) or a single *C. posadasii* endospore held with a micropipette (C). Each panel is a composite of three video images depicting the changes in neutrophil morphology in response to the placement of the pathogenic target at different sides of the cell. (**D**) The complement system in the serum of the host assembles complement complexes on the surface of foreign target particles (T). Some of these complexes, such as the C5 convertase, are enzymes that cleave other serum proteins and release anaphylatoxins, which are highly potent chemoattractants, such as C5a. The radial concentration profile of anaphylatoxins surrounding the target (color gradient) forms rapidly but has a limited spatial reach (37, 48). Neutrophils detect this anaphylatoxic cloud and respond by extending chemotactic pseudopods toward the target. (**E**) Example measurement of the time course of the mean fluorescence intensity (MFI) of the Ca^{2+} indicator Fluo-4 during pure chemotaxis of a human neutrophil toward a pipette-held zymosan particle (Z) and eventual phagocytosis of the particle. Included are bright-field and fluorescence images

taken at the time points numbered (1) to (6) in the MFI graph. The MFI remained low and essentially flat throughout the chemotaxis stage but exhibited a steep increase caused by a Ca^{2+} burst after the zymosan particle was brought into physical contact with the neutrophil (see also movies S1 to S3). Scale bars, 10 μm. au, arbitrary units.

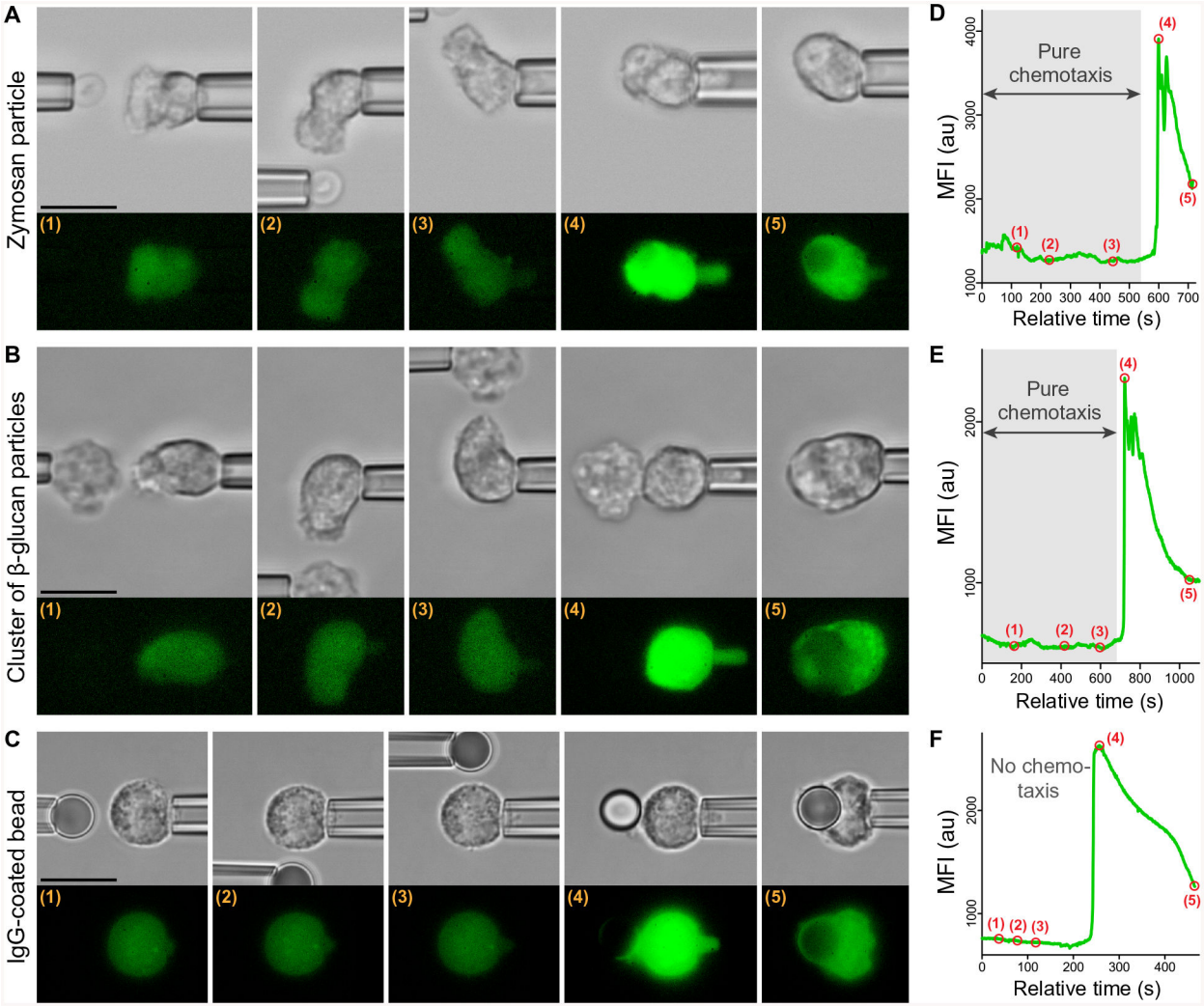

Fig. 2. Absence of Ca^{2+} bursts during pure chemotaxis.

Three representative examples show experiments that examined the response of individual pipette-held neutrophils to various targets using the dual-micropipette assay (Fig. 1E). (**A** to **C**) Filmstrips show both bright-field and fluorescence images of experiments in which the target (held in the left pipette in each image) was first placed near and eventually in contact with a neutrophil (held at the right in each image). The targets were zymosan particles (A), β-glucan particles (B), and an immunoglobulin G (IgG)–coated bead (C). The test with β-glucan (B) depicts an experiment using a cluster of β-glucan particles but is representative of experiments with both clusters and individual β-glucan particles. (**D** to **F**) The graphs show the time course of the MFI of Fluo-4 corresponding to the intracellular Ca^{2+} concentration during each experiment. The numbered points on the graphs mark the times at which the respective images (A to C) were taken. During single-cell experiments with the fungal model particles, the shown neutrophil behavior—chemotaxis without a Ca^{2+} burst followed by phagocytosis with a Ca^{2+} burst—was observed in 34 (of $n = 36$) experiments with zymosan (A and D) and in 16 (of $n = 19$) experiments with β-glucan particles (B and E). The shown neutrophil response to an antibody-coated bead—no chemotaxis but phagocytosis

that then triggered a Ca^{2+} burst (C and F)—was observed in all experiments with these beads (n = 43). See also movies S1 to S3. Scale bars, 10 μm.

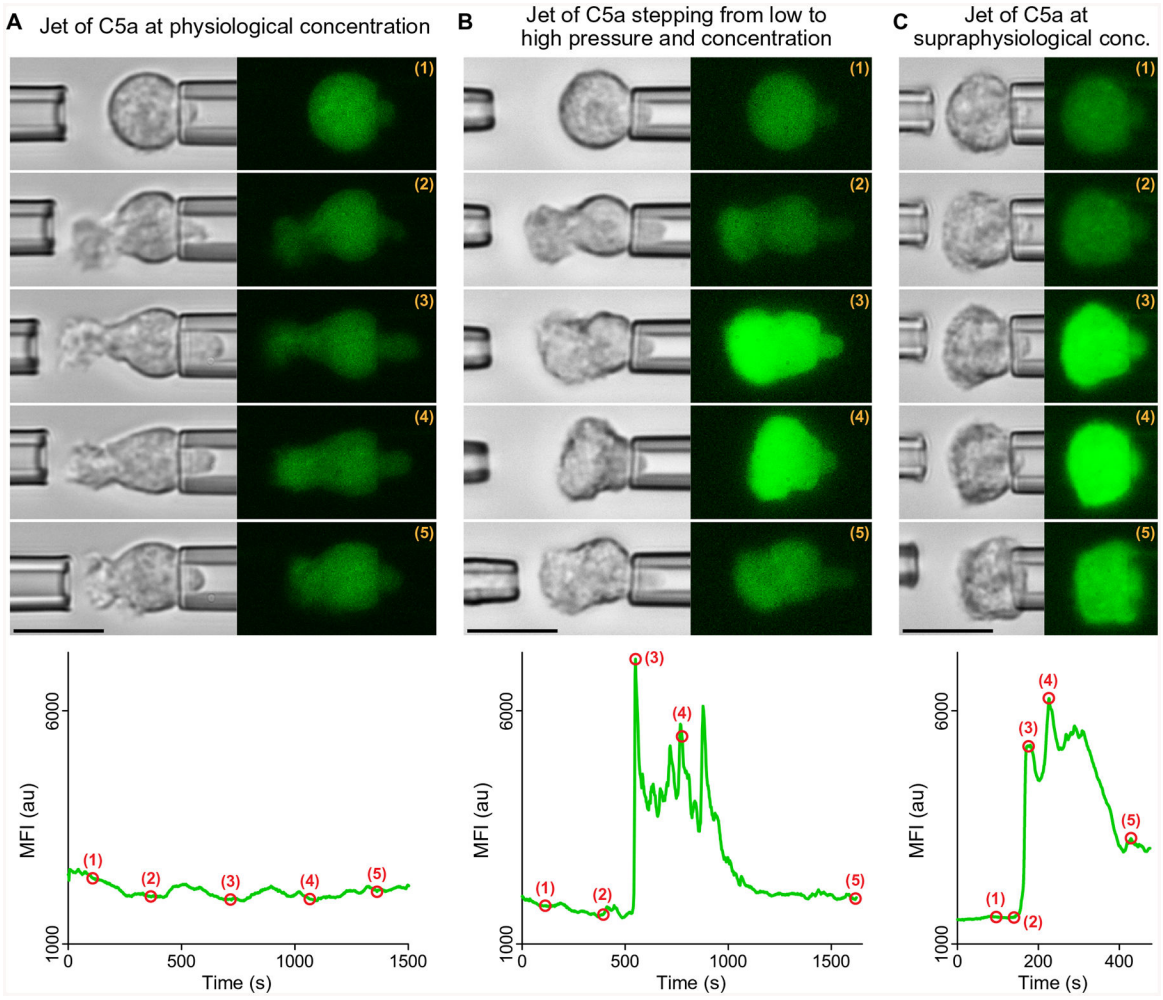

Fig. 3. Supraphysiological concentrations of C5a or costimulation by shear flow can trigger Ca^{2+} bursts in nonadherent neutrophils.

Three representative examples show experiments in which jets of C5a solutions were ejected from the left micropipette toward neutrophils held with the right pipette. Filmstrips of bright-field and fluorescence images show snapshots of the neutrophil response at the time points marked by numbers in the included graphs of the MFI of Fluo-4. (**A**) The neutrophil responded to a jet of a 0.1 nM C5a solution by extending a chemotactic pseudopod for more than 25 min, during which time no Ca^{2+} burst occurred. This example is representative of n =19 single-cell experiments. (**B**) The neutrophil was subjected to a jet of a 10 nM C5a solution. The jet was initially applied with a low pressure over a distance of 7 μm, inducing the extension of a pseudopod (time points 1 and 2). After about 9 min, a fivefold increase of the pipette pressure triggered a Ca^{2+} burst, accompanied by a cell contraction in the horizontal direction (time points 3 and 4). After temporary removal of the left pipette, a low-pressure jet was applied once more (time point 5), causing the cell to resume the protrusion of a directed pseudopod. This example is representative of n =16 single-cell experiments in which C5a jets induced Ca^{2+} bursts in chemotaxing cells. (**C**) Application of a low-pressure, 0.1 μM C5a jet from a short distance triggered a Ca^{2+} burst in a pipette-held neutrophil without previous pseudopod extension. In response, the cell appeared to flatten against the

pipette (time point 5). This example is representative of $n = 10$ single-cell experiments. Movie S4 combines single-live-cell videos of the three example experiments included in this figure. Scale bars, 10 μm.

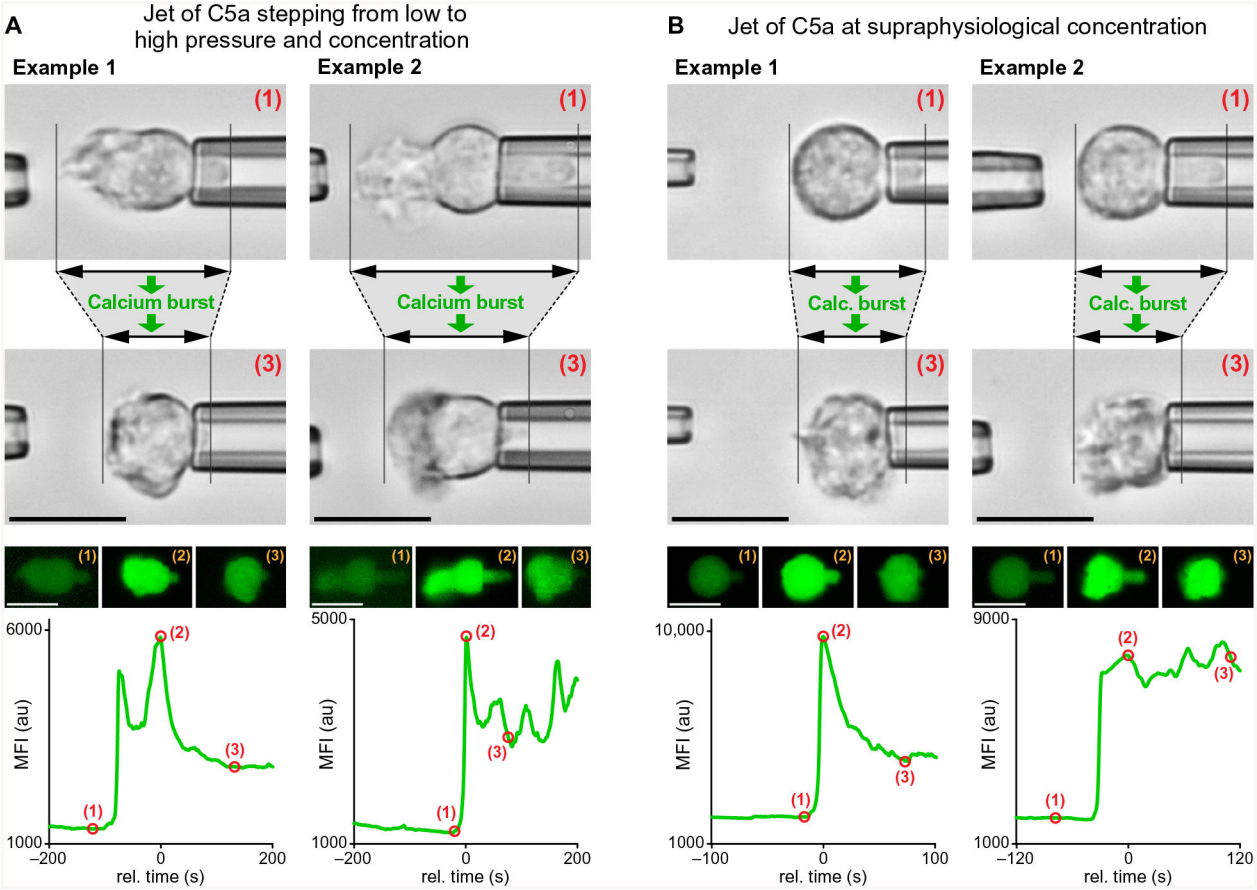

Fig. 4. Coincidence of Ca^{2+} bursts and axial cell contraction.

Representative examples of jet experiments in which C5a solutions were ejected from the left micropipette toward neutrophils held with the right pipette. The bright-field and fluorescence images show the changes of the neutrophil morphology that accompanied Ca^{2+} bursts during two different types of cell response, each illustrated with two examples. The images were taken at the time points marked by numbers in the graphs of the MFI of Fluo-4. (**A**) Initially chemotaxing neutrophils were subjected to a sudden increase of the jet pressure, which also increased the C5a concentration at their surface. The resulting Ca^{2+} bursts coincided with a contractile morphology change of the cells in the horizontal direction (time points 2 and 3). (**B**) Sudden exposure of neutrophils to jets of supraphysiological concentrations of C5a triggered Ca^{2+} bursts that coincided with a contractile morphology change of the cells. The cells did not extend chemotactic pseudopods in this case. We observed the illustrated behavior—Ca^{2+} bursts that were accompanied by a decrease or arrest of the total axial cell extension—in 24 (of n =26) single-cell experiments. Detailed time courses of such cell contractions are shown in fig. S3. Scale bars, 10 μm.

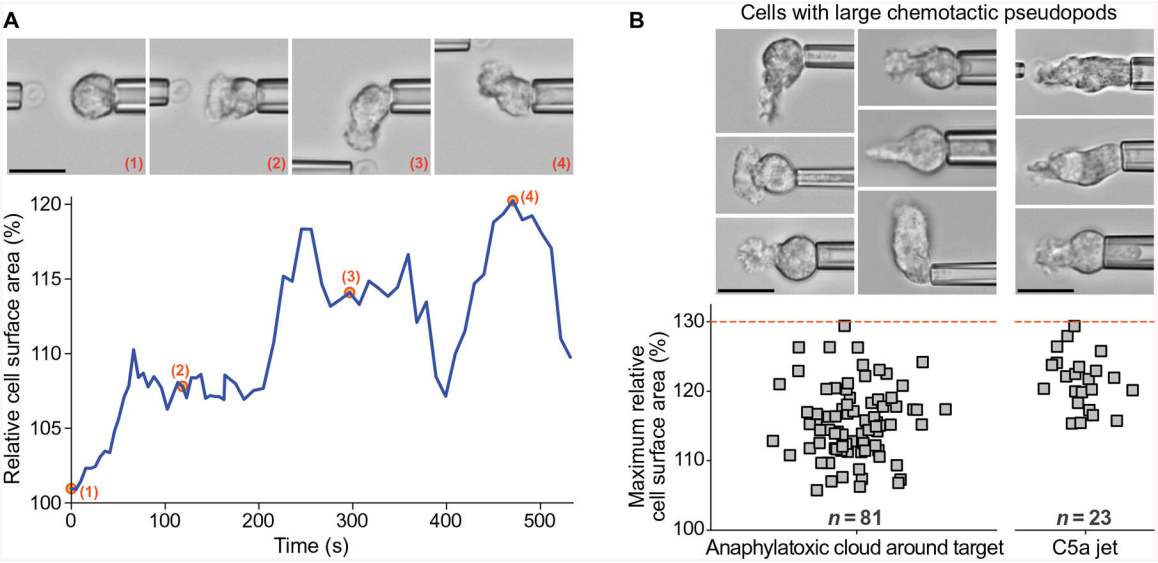

Fig. 5. Limited surface area expansion during pure chemotaxis.

(**A**) The graph shows an example of the time-dependent surface area of a neutrophil during pure chemotaxis toward a pipette-held zymosan particle. Representative video snapshots were taken at the time points marked by numbers. (**B**) The column scatter plots show the values of the maximum cell surface area measured during pure chemotaxis in previous and current experiments with target particles (n =81) and during current jet experiments (n =23), respectively. The upper limit of these values is indicated by a dashed red line. Example videomicrographs of cells extending large chemotactic pseudopods are included. Our approach to measuring the cell surface area is illustrated in fig. S4. Scale bars, 10 μm.